Macromolecules

ARTICLE

pubs.acs.org/Macromolecules

Controllable-Induced Crystallization of PE-*b*-PEO on Carbon Nanotubes with Assistance of Supercritical CO_2: Effect of Solvent

Ning Yu, Xiaoli Zheng, Qun Xu,* and Linghao He

College of Materials Science and Engineering, Zhengzhou University, Zhengzhou 450052, People's Republic of China

ABSTRACT: As a typical double-crystalline diblock copolymer, polyethylene-*b*-poly(ethylene oxide) (PE-*b*-PEO) has been successfully modified on single-walled carbon nanotubes (SWCNTs) and multi-walled carbon nanotubes (MWCNTs) using a simple supercritical carbon dioxide (SC CO_2) antisolvent-induced polymer epitaxy method. The characterization results of transmission electron microscopy (TEM) demonstrated that the unique double-crystalline block copolymer PE-*b*-PEO can be periodically decorated along carbon nanotubes (CNTs), leading to a novel amphiphilic nanohybird structure. The effect of different solvents on the decorated patterns of PE-*b*-PEO on CNTs has been discussed in this work. We found that the selectivity of solvent to the segments of block copolymer played a decisive role on the morphology of PE-*b*-PEO assembling on CNTs. When 1,2-dichlorobenzene (DCB) or *p*-xylene was used as the solvent, PE-*b*-PEO formed periodic patterns on CNTs, where the nanotube-induced PE crystallization was critical to the formation of the novel regular nanohybird structure. When the solvent was switched to *N*,*N*-dimethylacetamide (DMAc), which was more selective for PEO, periodic patterns were not observed, and merely the thin polymer coatings were observed on CNTs. The experimental results indicated that the decorating degree of PE-*b*-PEO on the surface of CNTs increased significantly with the increase of SC CO_2 pressure. FT-IR and Raman spectra indicated that there existed multiple weak molecular interactions between polymer chains and CNTs. Therefore, we anticipate this work may lead to a controllable method making use of peculiar properties of SC CO_2 to help to fabricate the functional CNTs-based nanocomposties containing diblock copolymer with the various micromorphologies in the different organic solvents.

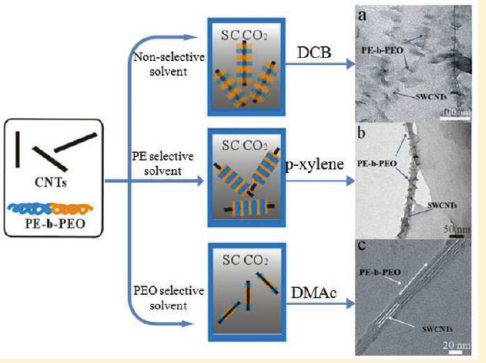

1. INTRODUCTION

Over recent years carbon nanotubes (CNTs) have become the focus of considerable research owing to their exciting potential applications in nanocomposites, molecular devices or advanced materials with their extraordinary mechanical strength, thermal conductivity, and electronic and optical properties.[1−3] However, significant effort is required in order to resolve the obstacle that the dispersion of CNTs in solvents and polymer matrixes due to the poor solubility and processability.[3] Using polymer chains to "wrap" CNTs is a versatile and effective way for the functionalization of CNTs.[4] Interest has been shown for CNTs' functionalization with polymers, such as polyethylene (PE),[5] poly(ethylene glycol) (PEG),[6] and poly(ether ether ketone) (PEEK)[7] because of their potential use in tissue engineering, packing materials, and thermoplastic devices, etc.[5−7]

Compared with homopolymers, block copolymers (BCPs) may provide a series of attractive noncovalent wrapping and decoration methods for the functionalization of CNTs.[4] BCPs can enhance the dispersibility and stability of CNTs in a wider range of organic solvents and the host polymer matrices. Recently, some groups have studied on the modification of CNTs with the amphiphilic block polymers. Li et al. have used spincoated method to fabricate PE-*b*-PEO/CNTs nanohybrid. They showed that judiciously selected crystalline block copolymers could be periodically decorated along carbon nanotubes, leading to amphiphilic, alternating patterns with a period of ∼12 nm.[8] Wang et al. used a controlled polymer crystallization method to decorate poly(vinylcyclohexane)-*b*-poly(ethylene)-*b*-poly(vinylcyclohexane) (PVCH−PE−PVCH) block copolymers on carbon nanotubes and formed a novel nanohybrid epitaxial brush structure, which consisted of a central CNT and disk-shaped folded chain lamellae of PE blocks with random coils of amorphous PVCH blocks.[4] Moreover, the dispersion of CNTs in the solvent with BCPs has attracted a lot of research interests. Rina et al. have had the careful study of the effect of adding different BCPs on the dispersion of CNTs and as well as their interaction in the selective solvent.[9−11]

Owing to the formation of unique aggregation morphology and the confined crystallization in the micro- and/or nanoscale self-assembled structure, the block copolymers can be self-assembled.[12−18] By the way, it is well-known that BCPs can present ordered self-assembled structures and can produce self-assembly behavior in selective solvents by means of the dual action: one block of the polymer has a close interaction with the selective solvent, while the other block is insoluble and tends to minimize their contact with the solvent.[19] So the selective solvent is an important factor to fabricate the self-assembly BCPs into a

Received: February 27, 2011
Revised: March 25, 2011
Published: April 29, 2011

regular morphology. Self-assemblies of BCPs in selective organic solvents have been studied previously by several groups.[20−23] Zhu et al. investigated the self-assembled crystalline−amorphous diblock copolymer and found the crystallization of crystallizable blocks can be efficiently confined within nanoenvironments.[20] Lodge et al.[21] and Chen et al.[22] have studied on the full phase behavior of block copolymers in solvents of varying selectivity. The topographical reconstruction of a BCP film was realized by Son et al. using vapor treatment with a selective solvent for each block.[23] Amphiphilic block polymers, such as polyethylene-*b*-poly(ethylene oxide) (PE-*b*-PEO), is a typical double-crystalline diblock copolymer, and it presents ordered self-assembled structures and confinement on crystallization.[24] Early work was reviewed by Sakurai et al.; they investigated the self-assembly and crystallization behavior of PE-*b*-PEO.[25] More recent results that bear relationship between morphological change and crystalline phase transitions of PE-*b*-PEO diblock copolymer are those of Cao et al.[26,27]

Supercritical fluids (SCFs) have attracted a great deal of interest in the synthesis and processing of materials due to their unusual properties such as low viscosity, high diffusivity, near-zero surface tension, and tenability.[28] Supercritical carbon dioxide (SC CO_2) is viewed as an excellent alternative to conventional organic solvents because it is inexpensive, nonflammable, and nontoxic and can be completely removed by simply lowering the pressure of the system.[29−32] The recent study of homopolymers modification on CNTs may help to enhance the understanding about decorated behavior of amphiphilic block copolymers on the surface of CNTs using the SC CO_2 anti-solvent-induced polymer epitaxy method (SAIPE method).[33−36] Thus, in this study, we aim to realize the modification of CNTs with PE-*b*-PEO block copolymers via the environmental benign SC CO_2-assisted method. Amphiphilic block polymers can self-assemble into specific structures on the surface of CNTs in selective solvents, and the amphiphilic block polymers/CNTs nanocomposites are expected to find their value in the development of novel compatilizer and surfactant for special materials.[37,38] Therefore, we anticipate this work can supply a clue about the achievement of various micromorphologies of the diblock polymer in different selective solvents with the assistance of SC CO_2, and accordingly the tailored nanohybrid structure is promising and important for functional design as a basic component in microfabrication and other correlating fields.

2. EXPERIMENTAL SECTION

2.1. Raw Materials. The single-walled carbon nanotubes (SWCNTs) were supplied by Carbon Nano Materials R&D Center, Chengdu Desran Technology Co., Ltd. (China), with a purity of 90 wt %. The multi-walled carbon nanotubes (MWCNTs) were purchased from Strem Chemicals, with a purity of 85 wt %. Polyethylene-*b*-poly(ethylene oxide) (PE-*b*-PEO) (molecular weight 1400 g mol^{-1}, 50 wt % PE) was purchased from Sigma-Aldrich. The organic solvents, such as *p*-xylene, 1,2-dichlorobenzene (DCB), and *N*,*N*-dimethylacetamide (DMAc) were purchased from Sinopharm Chemical Reagent Co., Ltd. (China). CO_2 with purity of 99.9% was provided by Zhengzhou Gas Co. (China).

2.2. Experimental Procedure. In a typical experiment, there were three basic steps to fabricate the PE-*b*-PEO/CNTs nanohybrids. First, PE-*b*-PEO (0.5 mg) was dissolved in *p*-xylene (3 g), at the suitable temperature (80 °C) close to the crystallization temperature of PE-*b*-PEO. CNTs (0.5 mg) were unbundled in *p*-xylene (2 g), and the mixture was ultrasonicated for 1 h at 45 °C before being added to the prepared PE-*b*-PEO solution. Second, the hybrid solution was transferred into the SC CO_2 apparatus (a 50 mL stainless steel autoclave) as quickly as possible. Before agglomeration of the unbundled CNTs, the CNT/polymer solution was quickly injected with CO_2 and CO_2 was charged into the autoclave up to the desired temperature and pressure. Third, the crystallization time was controlled for 3 h. At last, CO_2 was slowly released to atmospheric pressure, and the sample obtained was collected. Control samples with different solvents for PE-*b*-PEO and CNTs, including DCB and DMAc, were prepared in a similar manner.

Table 1. Solubility Parameters of PE-*b*-PEO and Three Organic Solvents

	PE	PEO	*p*-xylene	DCB	DMAc
solubility parameter/$(cal/cm^3)^{1/2}$	8.0	10.2	8.7	9.5	11.1

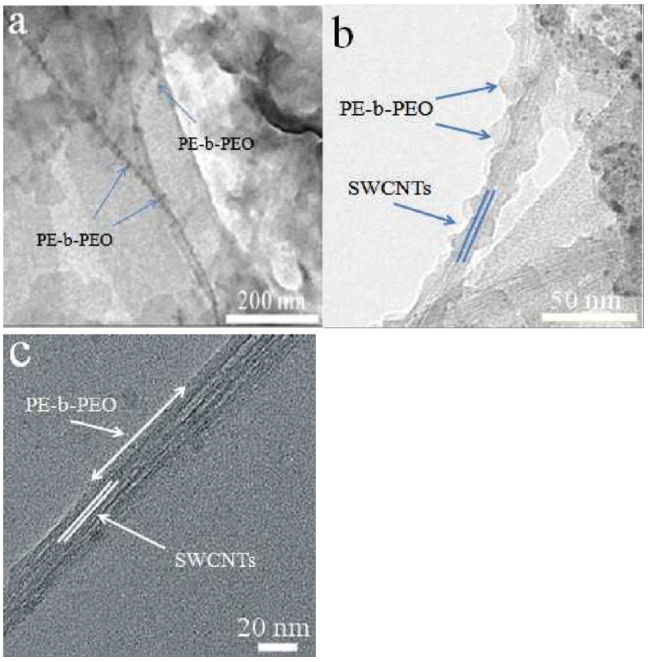

Figure 1. TEM images of the SWCNTs decorated with PE-*b*-PEO at 80 °C and 13 MPa for 3 h, but with different organic solvents: (a) DCB, (b) *p*-xylene, and (c) DMAc.

2.3. Characterization Methods. Transmission electron microscopy (TEM FEI Tecnai G^2 20) was used to observe the morphologies and microstructures of the decorated CNTs. Structural parameters of CNTs were characterized by IR spectra and Raman spectroscopy, respectively. IR spectra were acquired using a TENSOR 27 FTIR spectrometer (Bruker) in the absorption mode with 32 scans at a resolution of 2 cm^{-1} intervals. Raman spectra were collected on a Renishaw Microscope System RM 2000 at room temperature at 514.5 nm laser excitation. Spectra were collected at various locations for each sample studied to determine reproducibility.

3. RESULTS AND DISCUSSION

3.1. SWCNTs Modified with PE-*b*-PEO in Different Solvents with Assistance of SC CO_2. Amphiphilic block copolymers can present self-assembly behavior in selective solvents. The microstructure of block copolymer is controlled by the solvent selectivity for the different blocks: the soluble block tends to swell in the solvent, but the insoluble block tends to minimize

Scheme 1. PE-*b*-PEO Modification on CNTs with Assistance of SC CO_2 Using Three Different Solvents

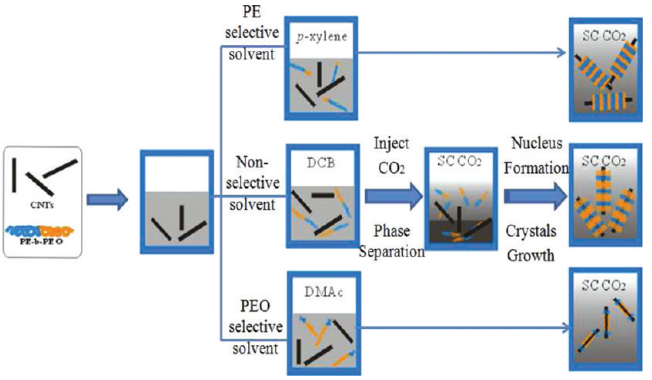

their contact with the solvent.[19] Owing to the high aspect ratio, CNTs are regarded as a good one-dimensional template to assembly inorganic nanoparticles.[3] Although many groups have investigated the self-assembly behavior of amphiphilic block polymers,[12−23] there is little study on the block polymers wrapping on CNTs in different selective solvents. Therefore, our study focused on the effect of different solvents on the morphology of amphiphilic block polymer (PE-*b*-PEO) and their different decorating patterning on CNTs using SAIPE method. In the SAIPE procedure, the variation of solvents is a typical peripheral factor, which affects the antisolvent power and results in different modification effects. Therefore, in this study, we choose three organic solvents such as *p*-xylene, DCB, and DMAc to study their effects on SC CO_2-assisted PE-*b*-PEO crystallization on CNTs. The solubility parameters of PE-*b*-PEO and the three organic solvents are supplied in Table 1. From Table 1, it can be found that the value of *p*-xylene is 8.7 $(cal/cm^3)^{1/2}$, which is close to those of PE (8.0), DMAc (11.1) is close to PEO (10.2), and DCB (9.5) is between PE (8.0) and PEO (10.2). Therefore, *p*-xylene and DMAc are selective solvent for PE segments and PEO segments, respectively. And DCB is a nonselective, but a good solvent for both blocks; i.e., both PE and PEO block chains can be soluble in it.

Figure 1 show the TEM images of PE-*b*-PEO/SWCNTs nanohybrids prepared in different solvents. We found that when DCB or *p*-xylene was used as the solvent, PE-*b*-PEO formed periodic patterns on CNTs, whereas merely the thin polymer coatings were observed on CNTs when using DMAc as the solvent. In addition, the periodic crystals modified on the surface of SWCNTs are more converged in *p*-xylene (Figure 1b) than in DCB (Figure 1a). These distinct results of the double crystalline block copolymer PE-*b*-PEO decorated on CNTs in different solvents motivate us investigate the main reason for the formation of various patterns on CNTs.

As block copolymers PE-*b*-PEO are dissolved in solvents, they will have the phase separation and form into ordered microstructures at a scale of 10−100 nm,[39] which can be considered as macromolecular surfactants.[40] Li et al. have investigated the possible scenarios in the block copolymer/nanotube/solvent interaction parameters: (i) the block copolymers form micelles or other aggregates, which separate from the CNTs; (ii) the block copolymers form micelles that wrap around the carbon nanotubes; and (iii) one segment of the block copolymer crystallizes on the carbon nanotubes, leading to nanotube-induced

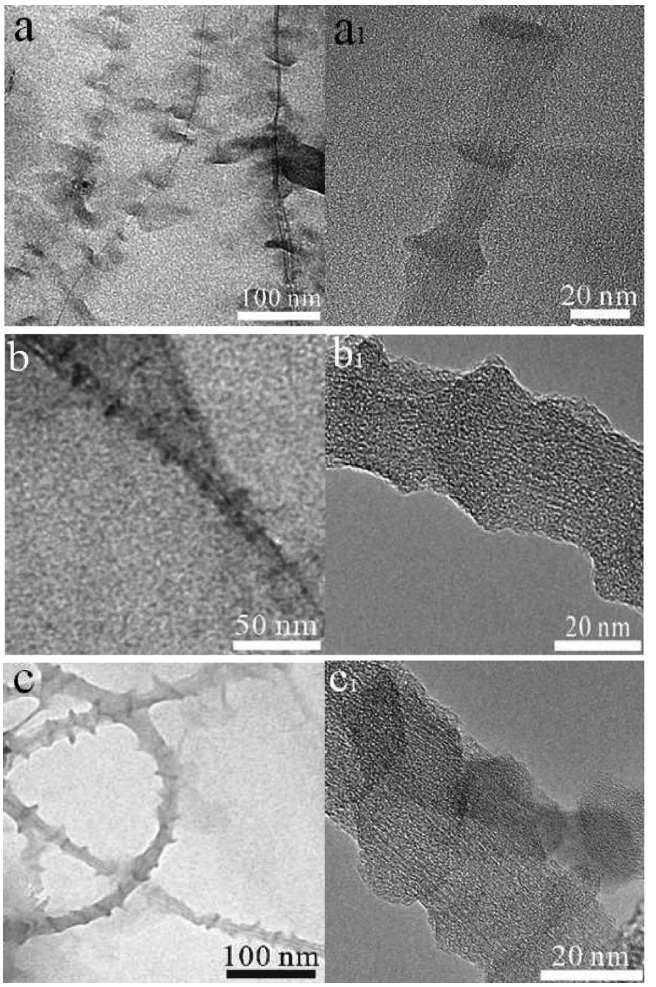

Figure 2. TEM images of the SWCNTs decorated with PE-*b*-PEO in DCB at 80 °C for 3 h, but with different experimental pressures: (a) and (a1) 11 MPa, (b) and (b1) 13 MPa, (c) and (c1) 15 MPa.

block copolymer phase separation.[8] In our study, the concentration of PE-*b*-PEO is only 0.1 mg/mL, which is much lower than the critical micelle concentration (CMC), at which PE-*b*- PEO individual chains could not aggregate.[12] So the scenario (iii) should be the domnant physical process in the present system.

The formation mechanism of PE-*b*-PEO assembling and modifying on CNTs with assistance of SC CO_2 in different solvents can be illustrated in Scheme 1. SC CO_2 cannot dissolve PE, but it can be miscible with DCB, *p*-xylene, and DMAc at suitable experimental conditions. Therefore, SC CO_2 is considered as the antisolvent for PE-*b*-PEO in the three different PE-*b*-PEO/solvent systems. This process can be described as follows. When CO_2 is injected into the PE-*b*-PEO/solvents system, the phase separation can be observed because of the reduced solvent strength, which leads to PE-*b*-PEO macromolecules separate out of the supersaturated solution successively. Further PE-*b*-PEO molecules can be adsorbed on the surface of CNTs. When DCB was used as the solvent, it is the nonselective for both segments of PE and PEO, but it is good solvent for both of them, so PE blocks and PEO block are in the extending state. With the injection of CO_2, the diblock copolymer can be separated out. Because of the CNTs can provide effective nucleation for PE segments, PE deposited on CNTs primarily and further realize its crystallization

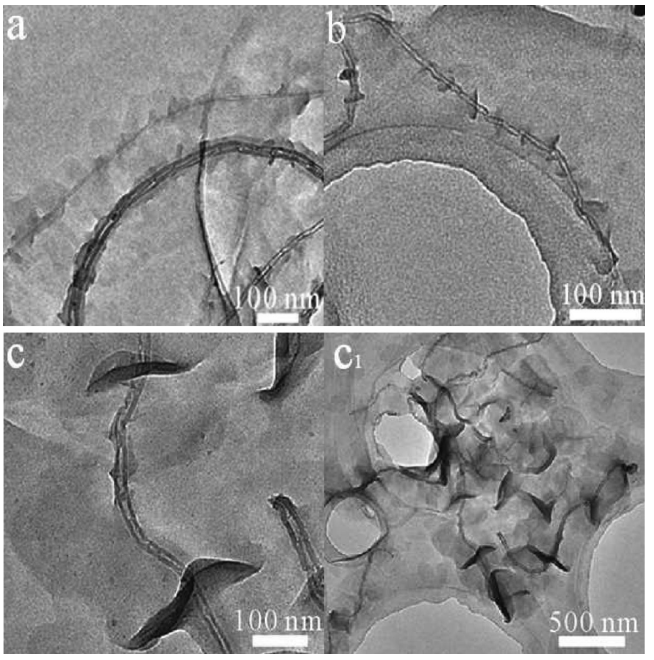

Figure 3. TEM images of the MWCNTs decorated with PE-*b*-PEO in DCB at 80 °C for 3 h, but with different experimental pressures: (a) 11 MPa, (b) 13 MPa, (c) and (c1) 15 MPa.

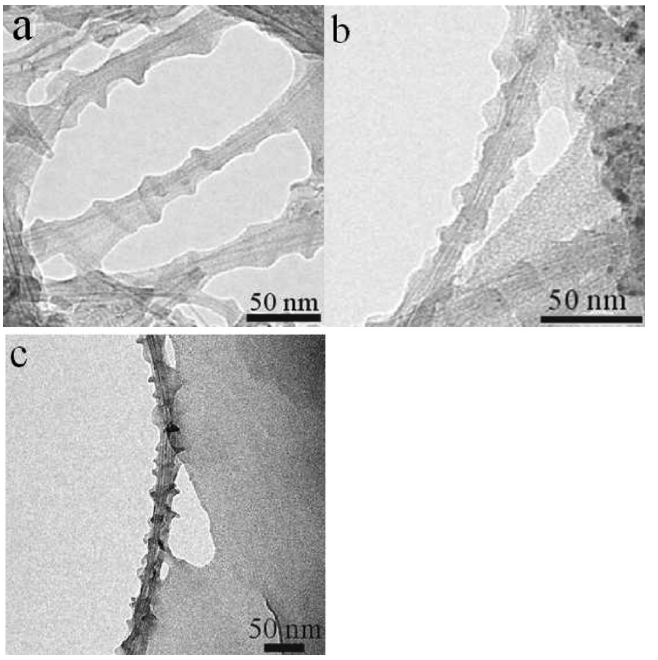

Figure 4. TEM images of the SWCNTs decorated with PE-*b*-PEO in *p*-xylene at 80 °C for 3 h, but with different experimental pressures: (a) 11 MPa, (b) 13 MPa, and (c) 15 MPa.

including the nucleus formation and crystal growth, whereas for the PEO segments, it has been reported that PEO did not crystallize on pristine CNTs because of the unfavorable interaction between CNTs and the PEO chains.[41,42] So the periodic patterns of PE-*b*-PEO on SWCNTs are obtained, which consist of disk-shaped folded chain lamellae of PE blocks with random coils of amorphous PEO blocks surrounding them (shown in Figure 1a). In the PE-*b*-PEO/SWCNTs/*p*-xylene system, because *p*-xylene is the selective solvent for PE, PE segments are in the stretching state while PEO block is in the curled state. Because of the effective heterogeneous nucleating role of CNTs on PE segments, PE chains can be easy to contact with SWCNTs. The curled PEO blocks may result in the decreased period between the adjacent PE lamellae (Figure 1b). When the solvent is switched to DMAc, which is more selective for PEO, thin PE-*b*-PEO coatings are formed on CNTs. In DMAc solvent, PE block is in the curled state, so PE segments are hard to adsorb on the surface of CNTs and conduct the heterogeneous nucleation. Therefore, the surface of SWCNTs is merely coated by a thin PE-*b*-PEO coating when using DMAc as solvent (Figure 1c).

Therefore, the large difference in morphological variation of PE-*b*-PEO decorating on CNTs can be attributed to the difference of the selective solvent. And the variation of solvent can induce the difference of the thermal mobility of PE segments in solvent, which is related with the conformation of chains and their packing mode, i.e., an extended chain or a folded chain. And this is a decisive factor on the obtained micormorphology of the assembling diblock copolymer on CNTs.

3.2. Modification of CNTs Using DCB as Nonselective Solvent for PE-*b*-PEO: Effect of CO_2 Pressure. PE-*b*-PEO assembling on CNTs in the form of periodic patterns when using DCB as solvent is evident from the TEM images of Figures 2 and 3. For supercritical fluid, experimental pressure has an important effect on the solvent power, and the variation of experimental pressure can be regarded as a typical outside effect.[34] Therefore, we are very interesting to investigate the effect of SC CO_2 on the decorated behavior of PE-*b*-PEO on CNTs. We changed the experimental pressure of SC CO_2 from 11 MPa to 13 and 15 MPa with the fixed concentration of PE-*b*-PEO at 0.01 wt % and CNTs concentration at 0.01 wt %. When the experimental temperature is 80 °C, the obtained TEM results of PE-*b*-PEO decorated on SWCNTs are shown in Figure 2. The surfaces of SWCNTs or SWCNT bundles are modified by PE-*b*-PEO regular patterns at different pressures. At low pressure of 11 MPa, the slice crystals are formed, and the period of regular pattern is ~20 nm. Whereas, with the increase of SC CO_2 pressure, we find that the period of the adjacent PE crystals is much smaller. This phenomenon is attributed to a variation of antisolvent power with the increase of SC CO_2 pressure.[6] Because of the dissolution of more CO_2, the volume of the liquid phase at higher pressure is more expanded, and the density and the solvent power of DCB rich phase decrease more. So more PE-*b*-PEO molecules can be separated out of the solvent to nucleate, which leads to the periods of PE lamellae on CNTs become smaller under the higher pressure.

Besides SWCNTs as the modification object, we also find a similar tendency that the modified effect of PE-*b*-PEO on multiwalled CNTs (MWCNTs) from 11 to 15 MPa at 80 °C (Figure 3). Apparently at 11 MPa, the crystals modified on MWCNTs are very thin and small. When the CO_2 pressure increases to 15 MPa, a more complete wrapping on MWCNT is observed, and the PE-*b*-PEO crystals can be observed much larger than that at 11 and 13 MPa. We attribute this phenomenon to the following reasons: with an increasing pressure of SC CO_2, the amount and speed of CO_2 dissolved in DCB increase and the solvent power of DCB decreases more; therefore, more PE-*b*-PEO can be deposited on MWCNTs and this supplies possibility to form larger crystals.

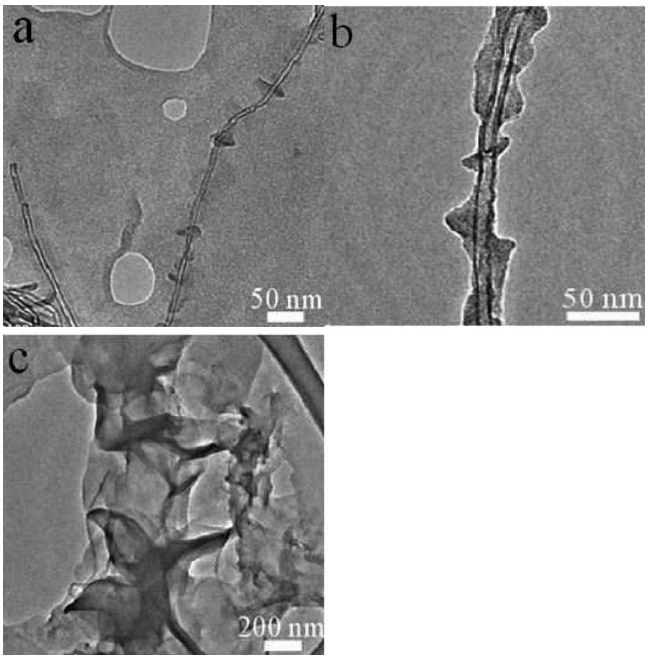

Figure 5. TEM images of the MWCNTs decorated with PE-*b*-PEO in *p*-xylene at 80 °C for 3 h, but with different experimental pressures: (a) 11 MPa, (b) 13 MPa, and (c) 15 MPa.

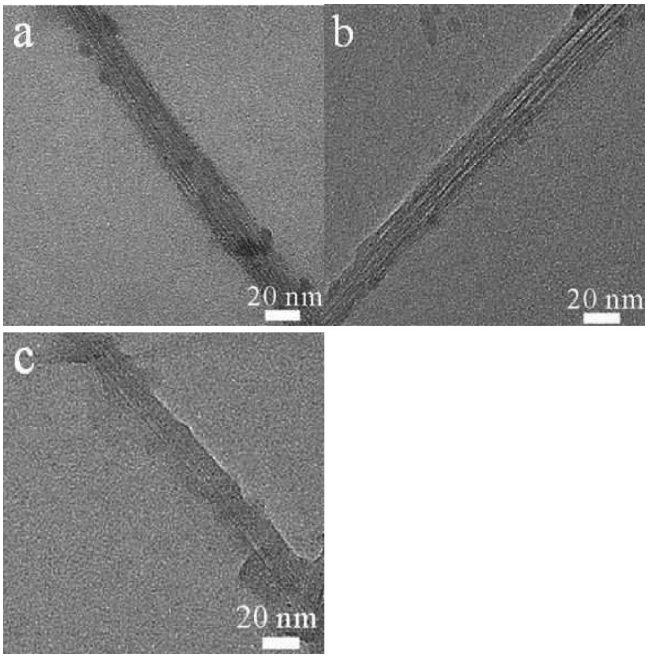

Figure 6. TEM images of the SWCNTs decorated with PE-*b*-PEO in DMAc at 80 °C for 3 h, but with different experimental pressures: (a) 11 MPa, (b) 13 MPa, and (c) 15 MPa.

3.3. Modification of CNTs Using *p*-Xylene and DMAc as Selective Solvent for PE-*b*-PEO: Effect of SC CO_2 Pressure. Figure 4 displays the TEM micrographs of SWCNTs decorated with PE-*b*-PEO using *p*-xylene as the solvent at different SC CO_2 pressures. Apparently, it can be seen that PE-*b*-PEO molecular chains have wrapped around CNTs with a regular pattern. With

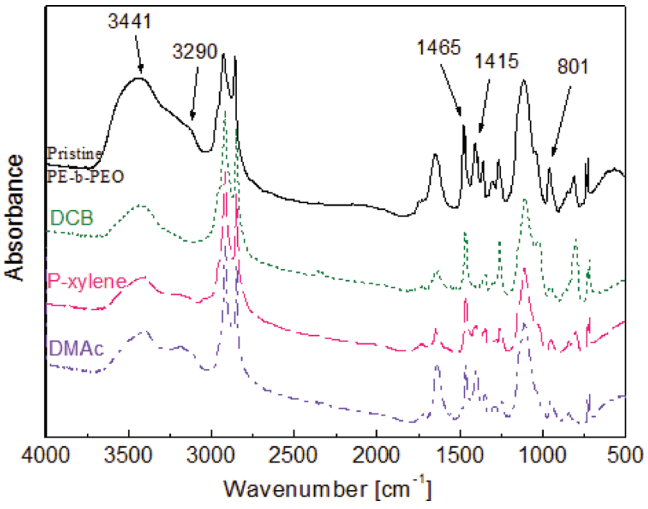

Figure 7. FTIR spectra of pristine-PE-*b*-PEO and PE-*b*-PEO decorating SWCNTs at SC CO_2 pressures of 13 MPa at 80 °C using different solvents: DCB, *p*-xylene, and DMAc for 3 h.

the change of pressure from 11 to 15 MPa, the crystals modified on the surface of SWCNTs are more converged. In addition, we use MWCNTs as nucleation center to study the modification effect of PE-*b*-PEO, shown in Figure 5. It is evident that with the increase of SC CO_2 pressure the sizes of the lamella are much larger. Further we study the effect of SC CO_2 pressure on the modification of diblock copolymer on CNTs using DMAc. The experimental results are shown in Figure 6, and it can be observed that the wrapping PE-*b*-PEO on CNTs is just thin polymer coatings no matter at any SC CO_2 pressure.

3.4. Interaction Analysis between CNTs and PE-*b*-PEO. In the early research, the $\pi-\pi$ interactions of CNTs which is considered as electron-rich molecules with electron-deficient molecules have been used for the noncovalent functionalization.[43,44] Recently, Kondratyuk et al. have shown that molecular interactions between carbon−hydrogen groups (CH groups) and π systems and the existence of CH$-\pi$ interactions could lead to adsorption.[45] Furthermore, Baskaran et al. have used the FTIR and Raman spectra to show the evidence for the presence of CH and OH group in molecules may form interactions with the π systems of MWCNTs.[46]

For the pristine PE-*b*-PEO (Figure 7), the peaks at 3441 and 3290 cm^{-1} are due to stretching vibration band of OH, the peaks at 1465 and 1415 cm^{-1} are due to in-plane deformation vibration band of CH, and the peak at 801 cm^{-1} is owing to out-plane deformation vibration band of CH. Obviously, there are two differences between pristine PE-*b*-PEO and PE-*b*-PEO/SWCNTs nanohybrids in the three different solvents. On the one hand, the deformation vibration band of CH at 1415 and 801 cm^{-1} of PE-*b*-PEO/SWCNTs nanohybrids prepared in DCB and *p*-xylene are obviously decreased compared with pristine PE-*b*-PEO; on the other hand, the stretching vibration band of OH at 3290 cm^{-1} of nanohybrids prepared in DMAc is obviously increased compared with pristine PE-*b*-PEO. The results can confirm that the presence of CH$-\pi$ interactions in the nanohybrids prepared in DCB and *p*-xylene, which would change the intensity of the CH deformation vibration of the polymer. What is more, the increased intensity of the peak at 3290 cm^{-1} assigned to the stretching vibration band of OH can confirm that the presence of OH$-\pi$ interactions between PE-*b*-PEO molecules and SWCNTs in DMAc. Therefore, there

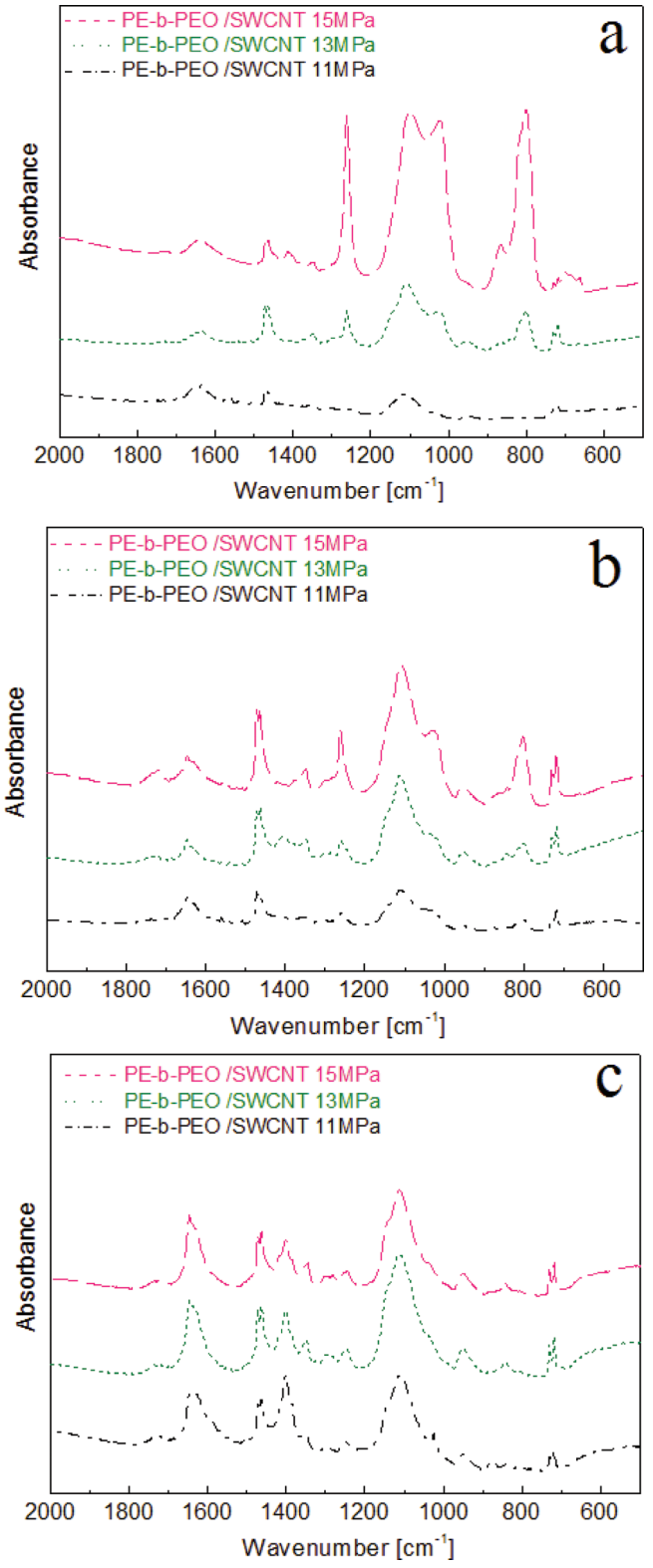

Figure 8. FTIR spectra of PE-*b*-PEO decorating SWCNTs at different SC CO_2 pressures of 11, 13, and 15 MPa using DCB (a), *p*-xylene (b), and DMAc (c) as solvent at 80 °C for 3 h.

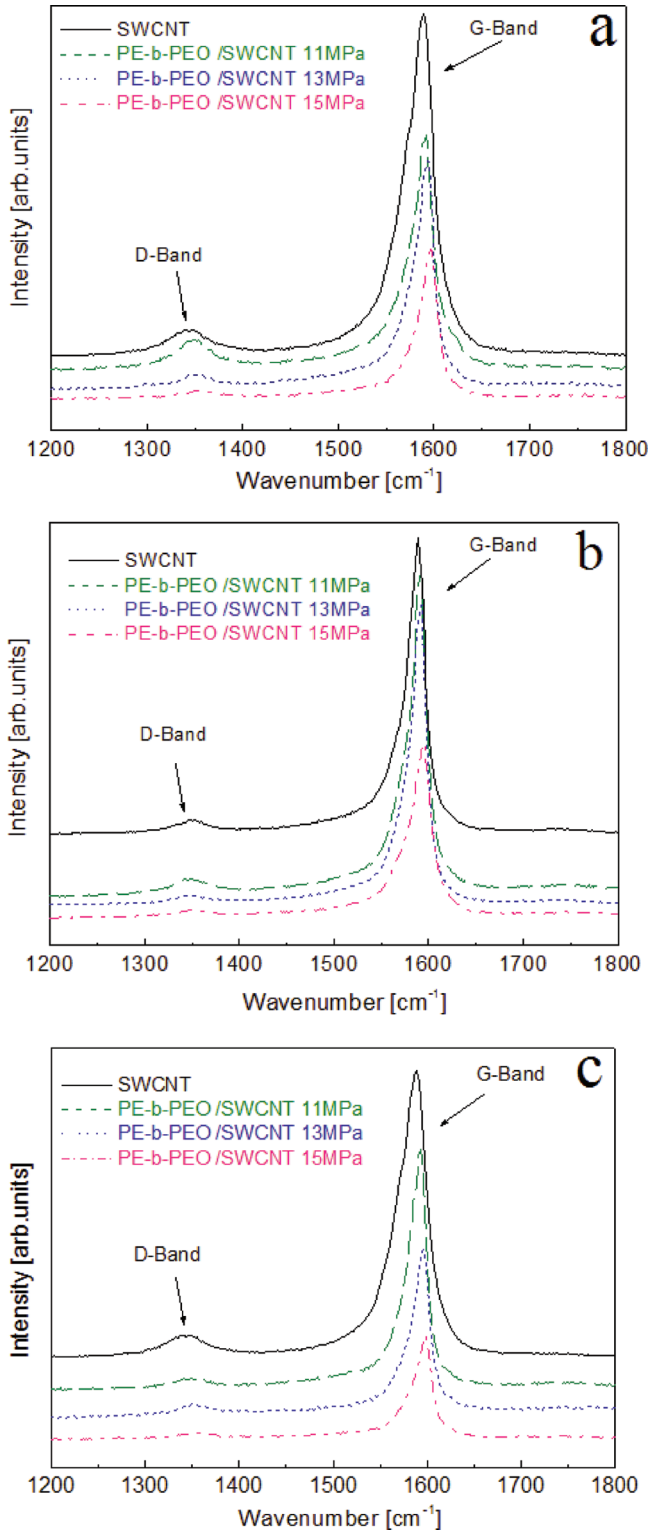

Figure 9. Raman spectra of pristine-SWCNTs and PE-*b*-PEO-decorated SWCNTs at 80 °C for 3 h and different SC CO_2 pressures: 11, 13, and 15 MPa using different selective solvents, DCB (a), *p*-xylene (b), and DMAc (c).

exist different interactions between PE-*b*-PEO molecules and SWCN4Ts in different solvents, CH$-\pi$ interactions in DCB and *p*-xylene, and OH$-\pi$ interactions in DMAc.

Figure 8 shows the FTIR spectra of PE-*b*-PEO/SWCNTs nanohybrids prepared under different SC CO_2 pressures in DCB (a), *p*-xylene (b), and DMAc (c). When the pressure is as low as 11 MPa, the absorption intensity of C$-$H deformation vibration

dx.doi.org/10.1021/ma200465a |*Macromolecules* 2011, 44, 3958–3965

Table 2. D- and G-Band Shifts and Raman I_D/I_G Intensity Ratios of Pristine SWCNTs and PE-*b*-PEO Decorating SWCNTs Using DCB as Solvent at 80 °C, with Different SC CO_2 Pressures of 11, 13, and 15 MPa

	D-band (cm^{-1})	G-band (cm^{-1})	I_D/I_G
SWCNTs	1347.2	1588.1	0.0523
DCB (11 MPa, 80 °C)	1349.3	1591.3	0.0631
DCB (13 MPa, 80 °C)	1351.3	1592.6	0.0647
DCB (15 MPa, 80 °C)	1352.7	1593.9	0.0672

Table 3. D- and G-Band Shifts and Raman I_D/I_G Intensity Ratios of Pristine SWCNTs and PE-*b*-PEO-Decorating SWCNTs Using *p*-Xylene as Solvent at 80 °C, with Different SC CO_2 Pressures of 11, 13, and 15 MPa

	D-band (cm^{-1})	G-band (cm^{-1})	I_D/I_G
SWCNTs	1347.2	1588.1	0.0523
p-xylene (11 MPa, 80 °C)	1349.1	1591.7	0.0642
p-xylene (13 MPa, 80 °C)	1352.3	1593.3	0.0673
p-xylene (15 MPa, 80 °C)	1353.1	1594.8	0.0688

bands of PE-*b*-PEO/SWCNTs nanocomposites is very weak due to only a few of PE-*b*-PEO molecules decorating on SWCNTs. With the increase of pressure, the C−H deformation vibration bands ascribed to PE-*b*-PEO are higher, confirming that more PE-*b*-PEO molecules are decorated on the surface of SWCNTs and the stronger noncovalent interactions between PE-*b*-PEO molecules and SWCNTs at the higher SC CO_2 pressure

In an attempt to further confirm the presence of CH−π interaction, the composite mixtures were subjected to Raman spectroscopy. Raman spectroscopy (RS) is convenient for analysis of the interfacial interactions between polymer and carbon materials, such as CNTs.[47] Figure 9 shows the Raman spectra of pristine SWCNTs and the PE-*b*-PEO-decorated SWCNTs nanohybrids produced in the three organic solvents under different SC CO_2 pressures, and the details of the results are provided in Tables 2−4. All carbon forms contribute to the Raman spectra in the range from 1000 to 1700 cm^{-1}. The observation of the two characteristic peak features at 1347.2 and 1588.1 cm^{-1}, corresponding to the D-band (C−C, the disordered graphite structure) and G-band (C═C, sp^2-hybridized carbon), respectively.[47] The intensity of the D- and G-bands of SWCNTs in the PE-*b*-PEO-decorated SWCNTs nanohybrids has a tendency to diminish with the increasing pressure of SC CO_2 (Figure 9). There are also some shifts in G-band and D-band peaks to higher wavenumber with the increasing pressure of SC CO_2 from 11 MPa to 13 and 15 MPa. The shift of the vibration frequency is attributed to the effect of CH−π or OH−π interactions between polymer molecules and the SWCNTs. In addition, with the increase of SC CO_2 pressure, SC CO_2 enhances the diffusivity of the polymers and more PE-*b*-PEO molecules can be separated out of the organic solvent. The more PE-*b*-PEO molecules in the nanohybrids increases the coverage area of polymer on SWCNTs' surface, which affects the vibration movements of C−C bands on the SWCNTs due to CH−π or OH−π interactions.[46] We also use I_D/I_G ratio, which is defined as the intensity ratio of the D-band to G-band of CNTs, to directly indicate the structure changes of CNTs.[48] As listed in Tables 2−4, the I_D/I_G ratio of pristine SWCNTs is 0.0523.

Table 4. D- and G-Band Shifts and Raman I_D/I_G Intensity Ratios of Pristine SWCNTs and PE-*b*-PEO-Decorating SWCNTs Using DMAc as Solvent at 80 °C, with Different SC CO_2 Pressures of 11, 13, and 15 MPa

	D-band (cm^{-1})	G-band (cm^{-1})	I_D/I_G
SWCNTs	1347.2	1588.1	0.0523
DMAc (11 MPa, 80 °C)	1351.6	1592.8	0.0634
DMAc (13 MPa, 80 °C)	1353.1	1594.4	0.0652
DMAc (15 MPa, 80 °C)	1354.7	1597.3	0.0698

Furthermore, the I_D/I_G ratio of the PE-*b*-PEO-decorated SWCNTs tends to be higher with the increasing pressure of SC CO_2. The enhancement of the I_D/I_G ratio can be attributed to the increase in sp^3-hybridized sidewall carbons due to the functionalization.

4. CONCLUSIONS

In this study, we have further developed the supercritical CO_2 antisolvent method to help a double-crystalline diblock copolymer, PE-*b*-PEO, to decorate on CNTs and further fabricate the functional nanohybrids of the PE-*b*-PEO/CNTs in three different solvents. When DCB or *p*-xylene was used as the solvent, PE-*b*-PEO formed periodic patterns on CNTs, where the nanotube-induced PE crystallization was critical to the formation of the novel regular nanohybird structure. When the solvent was switched to *N*,*N*-dimethylacetamide (DMAc), which was more selective for PEO, periodic patterns were not observed and merely the thin polymer coatings were observed on CNTs. The experimental results indicated that the decorating degree of PE-*b*-PEO on the surface of CNTs increases significantly with the increase of SC CO_2 pressure. FT-IR and Raman spectra indicate there are multiple weak molecular interactions between polymer chains and CNTs, where the CH−π interactions between PE-*b*-PEO and SWCNTs in DCB and *p*-xylene, and OH−π interactions in DMAc have been indicated, respectively. This work not only provides the possibilities of fabricating PE-*b*-PEO/CNTs nanocomposites with the assistance of SC CO_2 but also illustrates the vital effect of surface modification of CNTs in the different selective solvents. So combining the properties of SC CO_2 and diblock copolymer into one system is a novel field, and it may lead to the development of new method to control the surface modification of CNTs and other matrix materials by adjusting different organic solvent for diblock copolymer, which is a key step toward the achievement of the functional CNTs-based nanocomposties. And the tailored nanohybrid structures are promising as a basic component in microfabrication and other correlating fields.

AUTHOR INFORMATION

Corresponding Author

*E-mail qunxu@zzu.edu.cn; Tel +86 371 67767827; fax +86 371 67767827.

ACKNOWLEDGMENT

We are grateful for the National Natural Science Foundation of China (No. 20974102, 50955010) and the financial support from the Program for New Century Excellent Talents in Universities (NCET).

REFERENCES

(1) Baughman, R. H.; Zakhidov, A. A.; Heer, W. A. *Science* **2002**, *297*, 787–792.
(2) Vigolo, B.; Coulon, C.; Maugey, M.; Zakri, C.; Poulin, P. *Science* **2005**, *309*, 920–923.
(3) Wang, Z.; Liu, Q.; Zhu, H.; Liu, H.; Chen, Y.; Yang, M. *Carbon* **2007**, *45*, 285–292.
(4) Wang, W.; Xie, X.; Ye, X. *Carbon* **2010**, *48*, 1680–1683.
(5) Yue, J.; Xu, Q.; Zhang, Z. W.; Chen, Z. M. *Macromolecules* **2007**, *40*, 8821–8826.
(6) Zhang, Z. W.; Xu, Q.; Chen, Z. M.; Yue, J. *Macromolecules* **2008**, *41*, 2868–2873.
(7) Díez-Pascual, A. M.; Naffakh, M.; Gómez, M. A.; Marco, C.; Ellis, G.; Martínez, M. T.; Ansón, A.; Gonzá lez-Domínguez, J. M.; Martínez-Rubi, Y.; Simard, B. *Carbon* **2009**, *47*, 3079–3090.
(8) Li, B.; Li, L. Y.; Wang, B. B.; Li, C. Y. *Nature Nanotechnol.* **2009**, *4*, 358–362.
(9) Rina, S. C.; Ivonne, M.; Marc, F.; Veronica, F.; Daniella, G.; Rachel, Y. R. *Macromolecules* **2010**, *43*, 606–614.
(10) Rina, S. C.; Yael, L. K.; Einat, N. R.; Rachel, Y. R. *Langmuir* **2004**, *20*, 6085–6088.
(11) Rina, S. C.; Einat, N. R.; Baskaran, E.; Yael, L. K.; Igal, S.; Rachel, Y. R. *J. Am. Chem. Soc.* **2004**, *126*, 14850–14857.
(12) Li, T.; Wang, W. J.; Liu, R.; Liang, W. H.; Zhao, G. F.; Li, Z. Y.; Wu, Q.; Zhu, F. M. *Macromolecules* **2009**, *42*, 3804–3810.
(13) Huang, W. H.; Luo, C. X.; Zhang, J. L.; Yu, K.; Han, Y. C. *Macromolecules* **2007**, *40*, 8022–8030.
(14) Chen, Y. F.; Zhang, F. B.; Xie, X. M.; Yuan, J. Y. *Polymer* **2007**, *48*, 2755–2761.
(15) Hiroki, T.; Katsuhiko, F.; Takeshi, O.; Takayuki, O.; Masamitsu, M.; Katsuhiko, T.; Tomoo, S. *Polymer* **2006**, *47*, 8210–8218.
(16) Albuerne, J.; Márquez, L.; Müller, A. J. *Macromolecules* **2003**, *36*, 1633–1644.
(17) Sinturel, C.; Vayer, M.; Erre, R.; Amennitsch, H. *Macromolecules* **2007**, *40*, 2532–2538.
(18) Castillo, R. V.; Arnal, M. L.; Muller, A. J.; Hamley, I. W.; Castelletto, V.; Schmalz, H.; Abetz, V. *Macromolecules* **2008**, *41*, 879–889.
(19) Wang, G. J.; Liu, Y. D. *Macromol. Chem. Phys.* **2009**, *210*, 2070–2077.
(20) Zhu, L.; Cheng, S. Z. D.; Calhoun, B. H.; Ge, Q.; Quirk, R. P.; Thomas, E. L.; Hsiao, B. S.; Yeh, F.; Lotz, B. *J. Am. Chem. Soc.* **2000**, *122*, 5957–5967.
(21) Lodge, T. P.; Pudil, B.; Hanley, K. J. *Macromolecules* **2002**, *35*, 4707–4717.
(22) Chen, X.; Dong, B.; Wang, B.; Shah, R.; Li, C. Y. *Macromolecules* **2010**, *43*, 9918–9927.
(23) Son, J. G.; Bae, W. K.; Kang, H.; Nealey, P. F.; Char, K. *ACS Nano* **2009**, *12*, 3927–3934.
(24) Cho, D.; Kim, Y. J.; Erkey, C.; Koberstein, J. T. *Macromolecules* **2005**, *38*, 1829–1836.
(25) Sakurai, S.; Hashimoto, K.; Fetters, L. J. *Macromolecules* **1995**, *28*, 7947–7949.
(26) Cao, W.; Tashiro, K.; Hanesaka, M.; Takeda, S.; Masunaga, H.; Sasaki, S.; Takata, M. *J. Phys. Chem. B* **2009**, *113*, 2338–2346.
(27) Cao, W.; Tashiro, K.; Masunaga, H.; Sasaki, S.; Takata, M. *J. Phys. Chem. B* **2009**, *113*, 8495–8504.
(28) Liu, Z. M.; Han, B. X. *Adv. Mater.* **2009**, *21*, 825–829.
(29) Khlobystov, A. N.; Britz, D. A.; Wang, J.; O'Neil, A. S.; Poliakoff, M.; Briggs, G. A. D. *J. Mater. Chem.* **2004**, *14*, 2852–2857.
(30) Desimone, J. M. *Science* **2002**, *297*, 799–803.
(31) Kendall, J. L.; Canelas, D. A.; Young, J. L.; DeSimone, J. M. *Chem. Rev.* **1999**, *99*, 543–563.
(32) Johnston, K. P.; Shah, P. S. *Science* **2004**, *303*, 482–483.
(33) Zhang, F.; Zhang, H.; Zhang, Z. W.; Chen, Z. M.; Xu, Q. *Macromolecules* **2008**, *41*, 4519–4523.
(34) He, L. H.; Zheng, X. L.; Xu, Q. *J. Phys. Chem. B* **2010**, *114*, 5257–5262.
(35) Li, Z. P.; Guan, H. T.; Yu, N.; Xu, Q.; Imae, I.; Wei, J. Y. *J. Phys. Chem. C* **2010**, *114*, 10119–10125.
(36) Yu, N.; He, L. H.; Ren, Y. Y.; Xu, Q. *Polymer* **2011**, *52*, 472–480.
(37) Kim, S. H.; Jo, W. H.; Kim, J. *Macromolecules* **1996**, *29*, 6933–6940.
(38) Kong, H.; Gao, C.; Yan, D. Y. *J. Mater. Chem.* **2004**, *14*, 1401–1405.
(39) Cheng, J. Y.; Ross, C. A.; Smith, H. I.; Thomas, E. L. *Adv. Mater.* **2006**, *18*, 2505–2521.
(40) Kang, Y.; Taton, T. A. *J. Am. Chem. Soc.* **2003**, *125*, 5650–5651.
(41) Wang, B. B.; Li, B.; X, J.; Li, C. Y. *Macromolecules* **2008**, *41*, 9516–9521.
(42) Zheng, X. L.; Xu, Q. *J. Phys. Chem. B* **2010**, *114*, 9435–9444.
(43) Klopman, G. *J. Am. Chem. Soc.* **1968**, *90*, 223–234.
(44) Stan, G.; Bojan, M. J.; Curtarolo, S.; Gatica, S. M.; Cole, M. W. *Phys. Rev. B* **2000**, *62*, 2173.
(45) Kondratyuk, P.; Yates, J. T. *Chem. Phys. Lett.* **2004**, *383*, 314–316.
(46) Baskaran, D.; Mays, J. W.; Bratcher, M. S. *Chem. Mater.* **2005**, *17*, 3389–3397.
(47) Athalin, H.; Lefrant, S. *J. Raman Spectrosc.* **2005**, *36*, 400–408.
(48) Yang, Q.; Pan, X. J.; Huang, F.; Li, K. C. *J. Phys. Chem. C* **2010**, *114*, 3811–3816.